Prepared for submission to JINST

Cerium-doped Fused-silica Fibers as Wavelength Shifters VERSION 0

N. Akchurin,[a,1] **J. Damgov**[a] **F. De Guio,**[a] **G. Dissertori,**[c] **E. Kendir,**[b] **S. Kunori,**[a] **T. Mengke,**[a] **F. Nessi-Tedaldi,**[c] **S. Pigazzini,**[d] **Ş. Yaltkaya**[b]

[a] *Texas Tech University, Department of Physics and Astronomy, Lubbock, TX, 79409, USA*
[b] *Akdeniz University, Department of Physics, Antalya, 07070, Turkey*
[c] *ETH, Zürich, Switzerland*
[d] *???*

E-mail: nural.akchurin@ttu.edu

Abstract: As part of our continued R&D in radiation-hard scintillating and wavelength shifting fibers by doping fused-silica with cerium, we evaluated the performance of a Ce-doped fiber as wavelength shifter coupled to a CeF_3 crystal using electron beams at CERN. The pulse shape and collection efficiency were measured using irradiated (10 MRad) and un-irradiated fibers. In addition, we evaluated the light yield of additional Ce-doped fibers and explored the possibility of using these types of "hybrid" fibers for future precision timing applications in high-luminosity environment.

Keywords: Cerium, optical fibers, fused silica

[1] Corresponding author.

Contents

1 Introduction

Light emission by plastic scintillators typically degrades by half after a few MRads (a few 10 kGy). Our objective is to explore possible gains in radiation-hardness by doping fused-silica with inorganic "dyes" or rare-earth elements to produce scintillating and/or wavelength shifting fibers. Our experience [**? ? ? ? ?**] shows that clear (un-doped) fused-silica fibers survive large doses (O[10] MGy), and our preliminary results reported here, and those of others (for example, [**? ? ? ? ? ? ? ? ? ?**]), on doped fused-silica suggest that this approach is likely to result in meaningful progress because there has been accumulation of data complemented by improved understanding of radiation damage and light emission and absorption processes in these types of structures [**? ? ?**]. We described our results from the first two prototype fibers (so-called $S^{(1)}$ and $S^{(2)}$ fibers correspond to the Phase-I and -II fibers in this paper) in an earlier publication [**?**]. In this paper, we report on the performance of additional fibers, Phase-III, Phase-IV, and T14, and especially on their behavior under gamma irradiation. Clear fused-silica fiber containing no dopants was also included as benchmark. This fiber is the same fiber as in the active medium of CMS's forward calorimeter, and its radiation-hardness properties were well-studied and reported in scientific literature. All fibers reported here are produced by Polymicro Technologies[1].

2 Description of Fibers

The first large-scale (> 1 km) cerium-doped fiber production in this study was that of Phase-I fiber. The cerium-doped core was 60 μm in diameter and enveloped by a 200 μm diameter coaxial glass

[1]Polymicro Technologies is a subsidiary of Molex located in Phoenix, AZ, USA.

layer. The core preform was doped with cerium by a proprietary dissolving method, and the Ce:Si molar ratio was $\sim 10^{-3}$. Phase-II fiber was essentially the same as Phase-I except for a larger central core (150 μm dia.). This fiber was also produced at a large scale (~2 km) using standard industrial techniques.

The core of the Phase-III fiber was Ce-doped (370 μm dia.) but without a glass layer around it. This fiber was produced to evaluate the efficacy of the clear glass layers in Phase-I and -II fibers in terms of light transport. Phase-IV fiber was produced with a 15-μm thick Ce-doped ring around a 200-μm diameter clear fused-silica core. In addition, a 600-μm diameter glass outer layer was introduced to further improve light transmission. The T14 fiber's Ce-doped core (150 μm dia.) was surrounded by a high OH^- fused-silica layer (400 μm dia). In contrast, the outer layers in Phase-I and -II fibers were composed of low OH^- glass.

Table 1 summarizes the dimensions of core, glass, cladding, and buffer while Figure 5 shows the fiber cross-sectional images. Some performance characteristics of Phase-I and -II fibers that were measured with the high energy beams at Fermilab were reported in our first paper [**?**]: For example, the Phase-I optical attenuation length measured about 5.8 ± 0.7 m using 16 GeV electrons. The speed of light propagation was 19.50 ± 0.38 cm/ns and was found to be consistent with the previously reported values [**?** **?**]. When the tail of the pulse was modeled by a sum of two exponential functions, two decay constants were $\tau_1 = 20.8 \pm 5.4$, and $\tau_2 = 93.0 \pm 12.6$ ns. The contributions of these components to the total light emission (radioluminescence) turned out to be $23.9 \pm 5.3\%$ and $76.1 \pm 5.3\%$, respectively.

Table 1. All fibers were cladded with fluorinated acrylate and UV-cured acrylate buffer.

Fiber Name	Core OD [μm]	Glass OD [μm]	Clad OD [μm]	Buffer OD [μm]
Phase-I	60±7	200±6	230^{+5}_{-10}	350±15
Phase-II	150±20	400±10	430±10	550±30
Phase-III	370±8	-	400 ±8	550±15
Phase-IV	200(clear) 215(doped)	600±6	630±10	800±30
Clear fused-silica	600±10	-	630^{+5}_{-10}	800±30
T14	150±5	400±5	450±5	500±15

Experimental setup in the beam figure here...

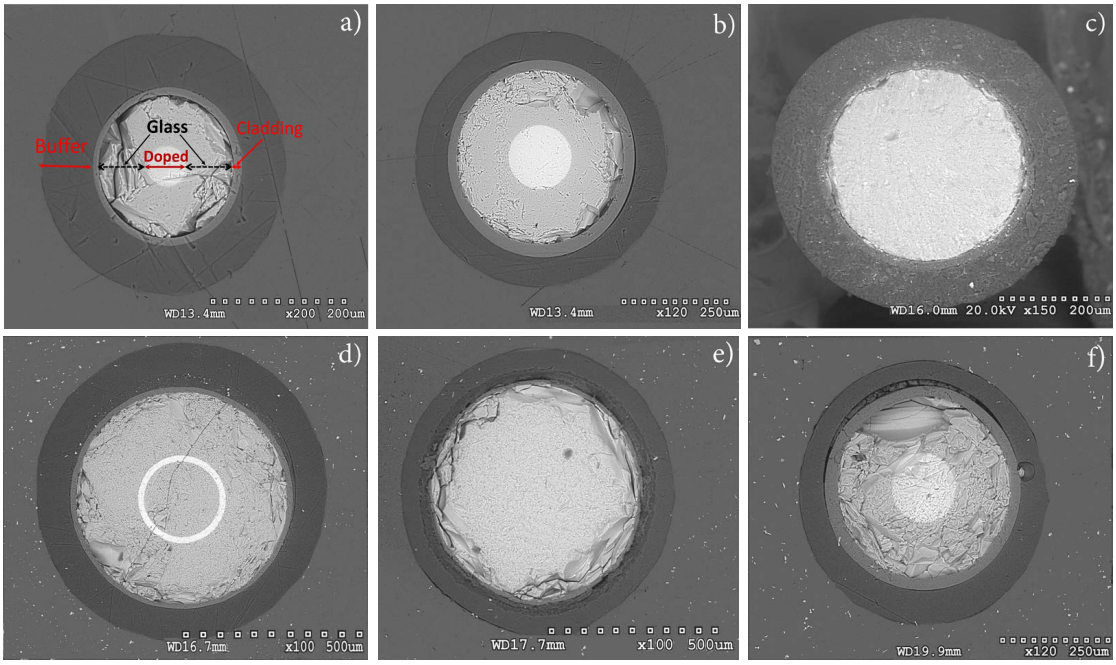

Figure 1. The cross-section of fibers *a)* Phase-I, *b)* -II, *c)* -III, *d)* -IV, *e)* clear fused-silica, and *f)* T14 are shown. The terminology used throughout the paper for different parts of the fiber is indicated on *a)*.

3 Scintillation Light Yield Measurements

The Phase-IV fibers were exposed to electron beam with energy of 16 GeV to measure their light yield. Bundle of 6 fibers were placed behind 4 cm brass absorber. The time characteristics of the Cerenkov(Q) and scintillation(S) light were used to separate and measure them individually. Then the S/Q ratio is compared to GEANT4 simulation with known scintillation light yield. This approach results in canceling out many of the systematic uncertainties related to the measurement of the individual components of the signal. For the unirradiated Phase-IV we measured S/Q=1.6 ± XX. This corresponds to 820 ± XX photons/MeV produced via radio-luminescence. For the irradiated Phase-IV fibers we observe reduced Cerenkov light production to about 63% and increased scintillation light yield by factor of 4.2. This corresponds to S/Q = 10.7 ± XX. When the tail of the signal is model by exponential function, the decay constants are 119.3 ± 20.7 ns and 102.3 ± 10.3 ns for unirradiated and irradiated fibers respectively.

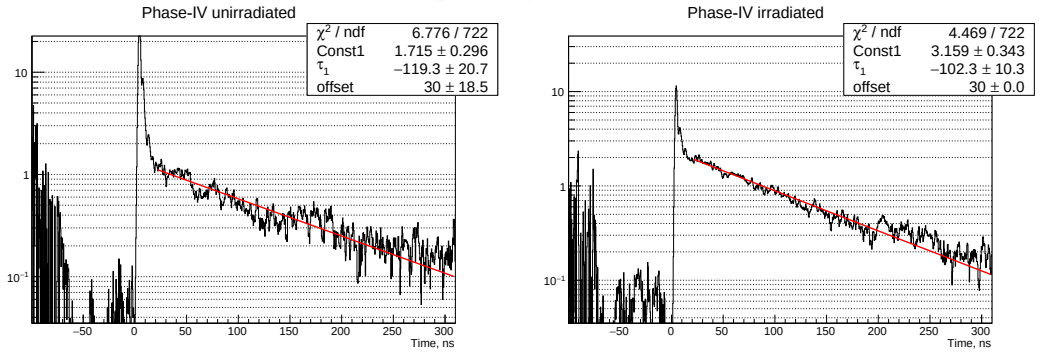

Figure 2. The average signal from Phase-IV unirradiated(left) and irradiated (right) fibers. The tail of the scintillation signal is well described by single exponent(red line) with time constant of 119.3 ± 20.7 ns and 102.3 ± 10.3 ns respectively.

R11864, phase4 unirradiated in front SPE 525.213 +/- 10.6236 Q [p.e] = 0.0924285 S [p.e] = 0.14725 S/Q = 1.59313

R11863, phase4 irradiate in front SPE 389.125 +/- 7.04617 Q [p.e] = 0.0578348 S [p.e] = 0.616969 S/Q = 10.6678

Geant4 prediction OD-ID=15um: Cerenkov : 0.131 p.e./evt Scintillation: 0.061 p.e./evt S/Q = 0.47 NB: G4 simulation has OD-ID = 15um for the ce-doped ring . In reality the OR-IR = 15um. Thus the S in this G4 setup is twice smaller and S/Q is twice lower than it should be - to be corrected if this G4 prediction is used. (JD - 18 Oct 2018)

4 Ce-doped Fibers Coupled to CeF_3 Crystal

A short paragraph on the CeF_3 crystal [**?**]

A figure on the absorption and emission lines of the CeF_3 crystal

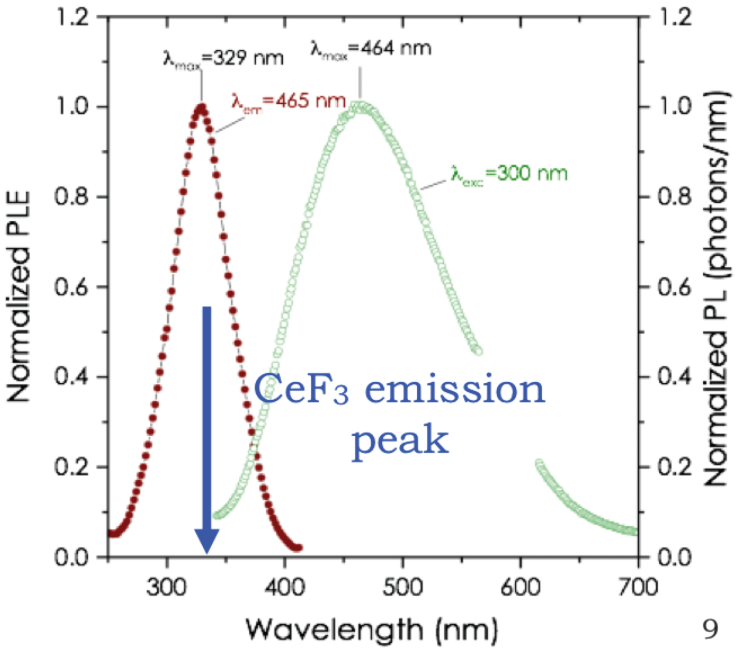

Figure 3. Spectrum.....

A figure on the fibers coupled to the CeF_3 crystal

Two sets of six fibers were air coupled to the larger of the crystal surfaces without optical grease and held in place by a tightly wrapped tyvek sheet as shown in Figure XXXX. One set of six consisted of un-irradiated and the other consisted of irradiated Phase-IV fibers that were viewed independently by photomultiplier tubes (Hamamatsu R6427). Irradiated fibers were subjected to 10 MRad of gamma irradiation three months prior to these measurements and some optical recovery had occurred. For cross calibration purposes between the two channels, the PMTs and the orientation of fibers on the crystal surfaces with respect to the beam direction were swapped in all possible (4) combinations. The PMT signals were read-out by a fast digitizer (CAEN V1742) at 5 GHz and a common trigger was generated by a fast multichannel photomultiplier (MCP). Figure 4 shows the measured spectra where the fast part (0-50 ns) of the spectra is clearly different and the irradiated fibers have lost sensitivity to this temporal region of light emission from the crystal. In the longer time scales (>50 ns), the tail of the signal is essentially the same (XX ns).

The following phenomena are responsible for this effect:

1. In the un-irradiated case (Figure XXX.a), the time structure of the CeF3 emission is evident. The pulse ...

2. In the irradiated case (Figure XXX.b), the fiber has lost its efficacy due to radiation damage and it is inefficient ...

3. Although the wavelength shifting by the irradiated fiber has been compromised, the total light level has seemingly increased as displayed in Figure XXX.c. The sensitivity of the irradiated fibers to the charged particles has actually gotten larger by a factor of four (?) (Section 3), accidentally compensating for the total signal but not the temporal features of the CeF3 light.

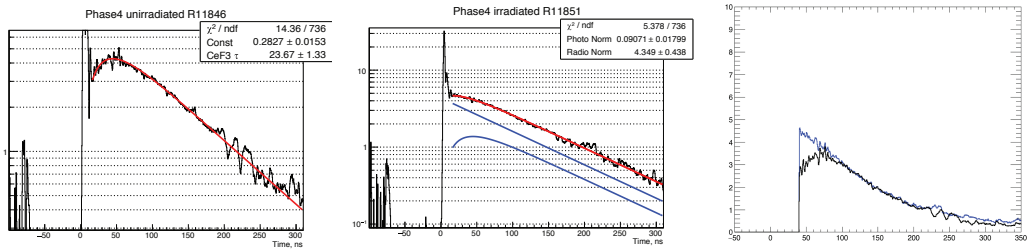

Figure 4. The averaged signals from the CeF_3 crystal coupled to either un-irradiated (left) or irradiated (middle) fibers display a significant difference at the short time scale (0-50 ns). The right plot shows the overlaid spectra when the two channels are calibrated for the same PMT gain. The red curve ... the blue curve...

4.1 Scintillation light analysis (temporary placeholder for text edits)

CeF_3 crystal with Phase-IV fibers attached to it were exposed to electron beam with energy of 16 GeV. The PMT signals were read-out by a fast digitizer (CAEN V1742) at 2.5 GHz and a common trigger was generated by a fast multichannel photomultiplier (MCP). Figure 4 shows the measured spectra where the fast part (0-50 ns) of the spectra is clearly different and the irradiated fibers have lost sensitivity to this temporal region of light emission from the crystal. In the longer time scales (>50 ns), the tail of the signal is essentially the same (XX ns). The scintillation light in this configuration has two components - photo-luminescence and radio-luminescence. The radio-luminescence results from particle passing trough the Ce-doped ring of the fibers. The timing characteristics of the two components of the scintillation signal differ due to the presence of comparable scintillation decay time in the CeF_3 crystal ($\sim 24ns$) in the photo-luminescence component. We use analytic functions to model the photo-luminescence and radio-luminescence contributions to the observed signal. We fit this model to the data to extract the relative contributions in the measured signal. The data from the unirradiated Phase-IV fiber is best described by model with $\sim$ 100% contribution from the photo-luminescence, while the data for irradiated Phase-IV fiber suggest that only a 1/4 of the total signal is from photo-luminescence. Furthermore we cross-reference this model prediction with the S/Q measurement without CeF_3 crystal and we found it to be in reasonable agreement, confirming sizable radio-luminescence contribution.

5 Timing Measurements

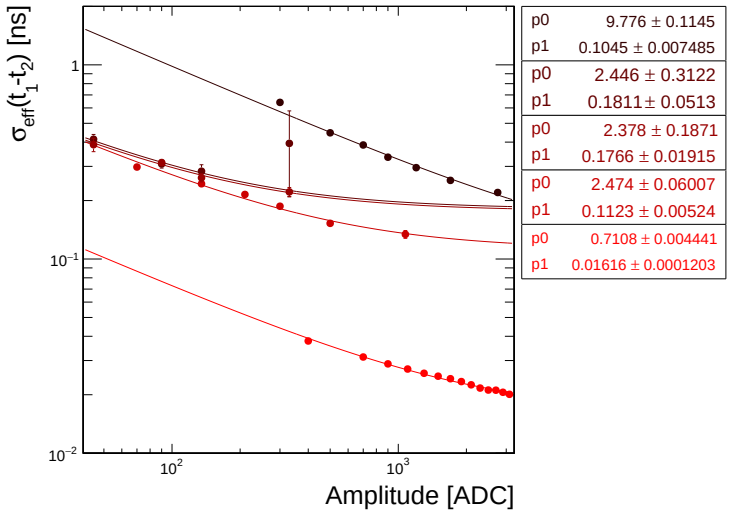

Figure 5. The timing resolution for ...

6 Conclusions

7 Acknowledgements

This work has been supported by the US Department of Energy, Office of Science (DE-SC001592), the Akdeniz University Scientific Research Projects Coordination Department (FDK-2017-2461), and the Scientific and Technological Research Council of Turkey, TÜBITAK, (No. 1059B141601412). We express our thanks to the AIDA2020 program and to Etiennette Auffray-Hillemanns for generously sharing the beam time at CERN. Jim Clarkin and Teo Tichindelean from Polymicro Technologies are thanked for their expertise, continued interest, and commitment to this R&D project.